Effects of π-conjugation-substitution on ESIPT process for oxazoline-substituted hydroxyfluorenes

Di Wang(汪迪)[1], Qiao Zhou(周悄)[1,2,†], Qiang Wei(魏强)[3], and Peng Song(宋朋)[1,‡]

[1] *Department of Physics, Liaoning University, Shenyang* 110036, *China*
[2] *College of Mathematics and Information Engineering, Chongqing University of Education, Chongqing* 400065, *China*
[3] *School of Science, Chongqing University of Technology, Chongqing* 400050, *China*

(Received 6 February 2022; revised manuscript received 8 April 2022; accepted manuscript online 11 April 2022)

Excited-state intramolecular proton transfer (ESIPT) molecules are broadly applied to UV absorbers, fluorescence sensing, and lighting materials. In previous work, the fluorescence colors of oxazoline-substituted hydroxyfluorenes and hydroxylated benzoxazole were diversified by adding the π-conjugation. There is intriguing that the mechanism of diversified fluorescence colors induced by ESIPT. Here, the density functional theory (DFT) and time-dependent DFT (TDDFT) are advised to identify the effects of π-conjugation on ESIPT and photophysical properties. The stabilized geometrical configurations, frontier molecular orbitals (FMOs) isosurfaces, and O–H stretching vibration frequency analysis demonstrate that PT processes are more active in S_1 state. Constructing the minimum energy pathways of ESIPT processes, we find that the calculated peak of enol and keto fluorescence of naphthoxazole (NO–OH) is distinctly bathochromic-shift relative to the oxazoline-substituted hydroxyfluorenes (Oxa–OH) configuration when adding π-conjugation-substitution, and it means that π-conjugation-substitution can diversify the fluorescence color. We hope our studies can establish new channels to devise the ESIPT-based molecules.

Keywords: density functional theory (DFT) and time-dependent DFT (TDDFT), excited-state proton transfer, intramolecular hydrogen bonding, π-conjugation-substitution

PACS: 82.39.Jn, 31.15.ee, 87.15.ht **DOI:** 10.1088/1674-1056/ac65f4

1. Introduction

Excited-state intramolecular proton transfer (ESIPT) molecules are extended applied in laser dyes, molecular switches, and fluorescent probes,[1–5] because of their distinguished characteristics like dual emission behavior and large Stokes shifts.[6,7] Since the ESIPT reaction in salicylate derivatives was reported by Weller,[8] the ESIPT reaction has attracted a lot of attention. Their investigative results show that ESIPT usually undergo a reversible four-step cyclic reaction process, that is to say, the transformation from normal to tautomer form.[9–11] According to this transformation, the chemical and physical properties of the molecule will change substantially, particularly the spectroscopic behavior. In recently years, lots of investigators have made numerous researches on the ESIPT reaction processes for developing and designing the innovative ESIPT molecules.[12–16] Therein, the introduction of substituent can make the ESIPT-based molecules have different properties. Ravikanth *et al.* showed that the substituent groups on tetraphenylethylene at the ortho position to benzothiazole have a great influence on the electronic structure.[17] Xu *et al.* found that substituted group could block the normal-tautomer tautomerism occurring through ES charge transfer.[18] Hasserodt *et al.* advised amino substituent could make the emission wavelengths shift to the deep red region.[19]

Recently, Nachtsheim's group successfully synthesized a series of ESIPT-based fluorenes oxazoline-substituted hydroxyfluorenes and hydroxylated benzoxazole, which could vary the emission colors.[20] Through altering the acceptor unit, they diversified the fluorescence recognition functions. However, their photophysical properties were blurry. Here, oxazoline-substituted hydroxyfluorenes (Oxa–OH), hydroxylated benzoxazole (BO–OH), and naphthoxazole (NO–OH) were selected. To elucidate the influence of substituent on ESIPT and photophysical properties, the density functional theory (DFT) and time-dependent density functional theory (TDDFT) are advised. By analyzing the mainly structural parameters of Oxa–OH, BO–OH, NO–OH and frequency analysis, the effects of under different substitution on the hydrogen bond strength were studied. In addition, the frontier molecular orbitals (FMOs), reduction density gradient (RDG) isosurfaces, and homologous potential energy surfaces (PESs) of these configurations were provided and analyzed, which can proclaim the direct information for the ESIPT process.

2. Calculation details

In this paper, the DFT and TD-DFT theories were advised to study the effect of substitution. All electronic structure calculations were provided by the 6-31+G(d) basis set, and B3LYP functional in Gaussian 09 program suite.[21–23] In addition, the integral equation formalism variant of the polar-

†Corresponding author. E-mail: zhouq@cque.edu.cn
‡Corresponding author. E-mail: songpeng@lnu.edu.cn

© 2023 Chinese Physical Society and IOP Publishing Ltd

izable continuum model (PCM) (IEFPCM) was selected.[25] Simultaneously, chloroform was taken into account, because the experiments were implemented in chloroform. In addition, the infrared (IR) vibrational frequencies of these stable geometries were carried out, and its results imply that there is no imaginary frequency, which penetrates that the computational geometries were at the local minimum point.[26,27] Then the deducted spectra of Oxa–OH, BO–OH, and NO–OH were calculated in view of the sustainable geometric configuration, and the calculated absorption and fluorescence spectrum is consistent with the experimental results. Furthermore, the FMOs and RDG were used to analyze the variation of intermolecular hydrogen bond strength by Multiwfn program suite.[28,29] Finally, their PESs were scanned to reveal transfer paths of hydrogen protons in different substitutions.

3. Results and discussion

3.1. Optimized geometric structures

Figure 1 show their optimized enol and keto configurations. Meanwhile, vibrational frequency analysis of these geometries are provided, which could assure the validity of these stable points. To clearly describe the important parameters of the hydrogen bonds, we numerically marked the atoms, and the related structure parameters are listed in Table 1. Interestingly, the calculative results uncover that the bond lengths of O_1–H_2 of these configurations are 0.999 Å, 0.991 Å, and 0.992 Å, while they change to be 1.016 Å, 0.997 Å, and 0.994 Å in the S_1 state, respectively. Thus, it can draw a conclusion that shortening of the O–H distance could be found with adding π-conjugation. In addition, the computational bond lengths of H_2–N_3 were 1.746 Å, 1.799 Å, and 1.796 Å in the S_0 state. When the molecules transfer to the S_1 state, the bond lengths vary to be 1.677 Å, 1.769 Å, and 1.786 Å. Clearly, the H_2–N_3 distance was shortened, which indicates that the intramolecular hydrogen bonds (O_1–$H_2\cdots N_3$) are strengthened in the S_1 state. In addition, the bond angle δ (O–H–N) varies from 146.86° , 145.66°, and 145.55° in the S_0 state to 149.27°, 147.42°, and 146.96° in the S_1 state for these structures. That is to say, the intramolecular hydrogen bonds in these configurations can be strengthened in excited electronic state.

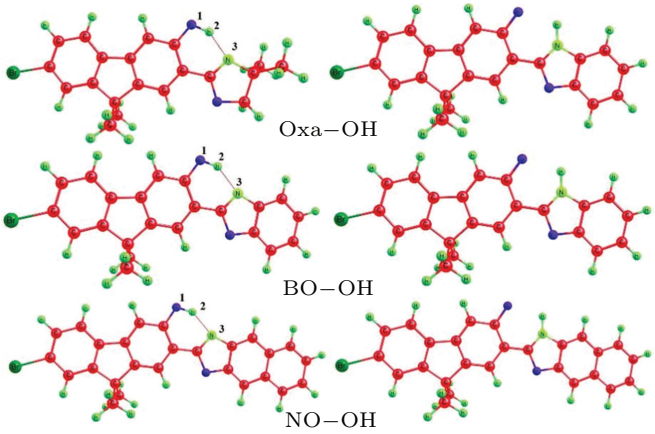


Fig. 1. Optimized geometries of NO–OH, BO–OH and Oxa–OH in the enol and keto-forms.

Table 1. The partial parameters of Oxa–OH, BO–OH and NO–OH in S_0 and S_1 states based on the DFT/TDDFT methods.

	Oxa–OH		BO–OH		NO–OH	
	S_0	S_1	S_0	S_1	S_0	S_1
O_1–H_1	0.999	1.016	0.991	0.997	0.992	0.994
H_1–N_2	1.746	1.677	1.799	1.769	1.796	1.786
δ (O_1–H_2–N_3)	146.86°	149.27°	145.66°	147.42°	145.55°	146.96°

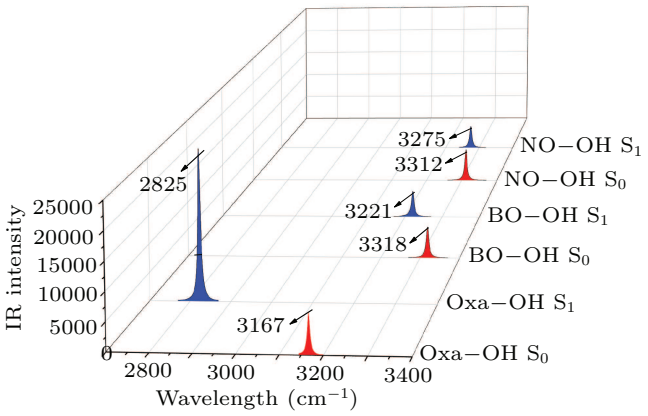


Fig. 2. Infrared vibrational spectra of Oxa–OH, BO–OH and NO–OH configuration in the S_0 and S_1 states.

Figure 2 represents the infrared spectra of O–H bands in the S_0 and S_1 states. It can be seen that the O–H stretching vibration frequencies for Oxa–OH, BO–OH and NO–OH are 3167 cm^{-1}, 3318 cm^{-1} and 3312 cm^{-1} in the S_0 state, respectively, and upon photoexcitation, it varies to 2825 cm^{-1}, 3221 cm^{-1} and 3275 cm^{-1} in the S_1 state. Overtly, the bathochromic-shift produced by hydrogen bond in the S_1 state could be found, which indicates that the intramolecular hydrogen bond is strengthened in the S_1 state.[30–32] Interestingly, the bathochromic-shift of 342 cm^{-1}, 97 cm^{-1}, and 37 cm^{-1} for the O–H stretching band was induced by the intramolecular hydrogen bonds of these structures, revealing that the difference value of hydrogen bond energy between S_0 and S_1 states decrease with π-conjugation.

3.2. Absorption and emission spectra

Figure 3 displays the computational electronic spectra of Oxa–OH, BO–OH and NO–OH configuration. It can be noted that their absorption peaks are at 334 nm, 382 nm and 387 nm,

which agree with the experimental results of 347 nm, 369 nm, and 372 nm, respectively. Besides, the calculated peak of normal fluorescence of these molecules were 377 nm, 445 nm, and 460 nm. A bathochromic-shift of 43 nm, 63 nm, 88 nm is relative to the absorption peak, which should be attributed to the Stokes shift. Distinctly, the bathochromic-shift is gradually increasing. In addition, it can be seen from Fig. 3 that another fluorescence peak is located at 467 nm, 486 nm, and 504 nm, which is ascribed to the keto-form of triple configurations.

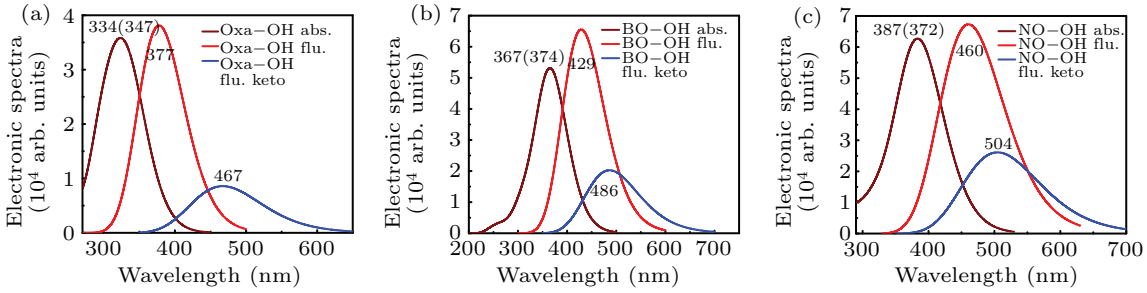


Fig. 3. Calculated absorption and fluorescence spectra of (a) Oxa–OH, (b) BO–OH and (c) NO–OH in chloroform solvent.

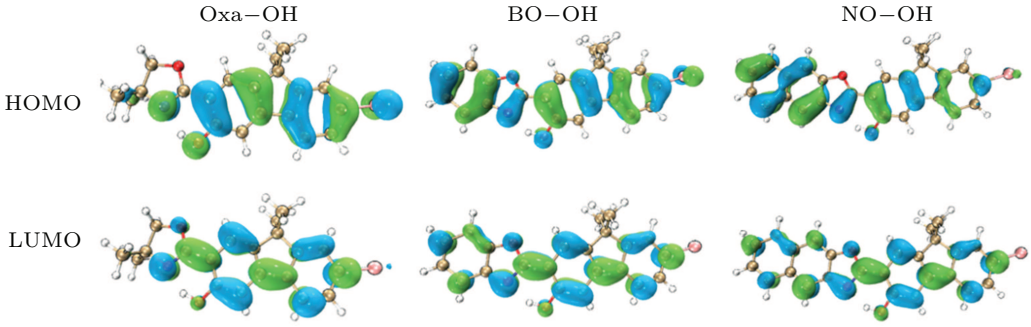


Fig. 4. The calculated frontier MOs of Oxa–OH, BO–OH and NO–OH.

Figure 4 shows the frontier MOs of the Oxa–OH, BO–OH and NO–OH, which could qualitatively discuss molecular configuration distribution and charge transfer in the S_1 state.[33,34] It is clear that the uniform distribution of charge on both sides of the molecular skeleton indicates that the charge transfer pattern of these configurations is typical π–π^* transition. The transfer of molecules from HOMO to LUMO shows obvious charge transfer characteristics. The charge distribution around N atom decreased significantly, while the charge distribution around O atom increased significantly, demonstrating the intramolecular hydrogen bond gradually strengthened, and thus promoting the occurrence of proton transfer process. These results show that the ESIPT process is due to intramolecular charge transfer. In Table 2, the HOMO and LUMO predominantly occupy the transition component with 94.6%, 97.8%, and 96.5% from the S_0 to S_1 state for Oxa–OH, BO–OH, and NO–OH, respectively. The relevant oscillator strength is 0.6919, 1.2700, and 1.3965, and the excitation energy is 334 nm, 367 nm, and 387 nm.

Table 2. Transition types with different excitation energies λ (nm) of Oxa–OH, BO–OH, and NO–OH respectively and their oscillator strengths (f) and transition compositions.

	Transition	λ (nm)	f	Composition	CI
Oxa–OH	S_1	334.07	0.6919	H→L	94.6%
BO–OH	S_1	367.06	1.2700	H→L	97.8%
NO–OH	S_1	387.24	1.3965	H→L	96.5%

3.3. Non-covalent interactions analysis

Figure 5 exhibited the obtained RDG isosurfaces, which can discern the influence of different substituents on the hydrogen bond strength in real space.[35–38] The strength of hydrogen bond interactions can be clearly described by analyzing $\rho(r)$ and RDG of the electron density. The RDG function can be indicated as

$$\mathrm{RDG}(r) = \frac{1}{2(3\pi^2)^{1/3}} \frac{|\nabla\rho(r)|}{\rho(r)^{4/3}}. \tag{1}$$

Additionally, the electron density matrix equation is obtained on the basis of Bader theory

$$\Omega(r) = \mathrm{sign}(\lambda_2(r))\rho(r). \tag{2}$$

Previous work shows that multiple weak interactions can be clearly found, namely, negative values of $\mathrm{sign}(\lambda_2)\rho$ refer to hydrogen bonding effects, positive $\mathrm{sign}(\lambda_2)\rho$ stands for steric effect and values near zero exhibit the van der Waals (VDW) interactions. We find that the spike peaks of these configurations are located at -0.048, -0.042 and -0.040 in the S_0 state. The interaction type is classified as hydrogen bond interaction, and the peak value is O_1–$H_2\cdots N_3$. Upon photoexcitation to the S_1 state, O_1–$H_2\cdots N_3$ shift to -0.056, -0.044 and -0.042, which promulgates that the hydrogen bond was strengthened in the S_1 state.

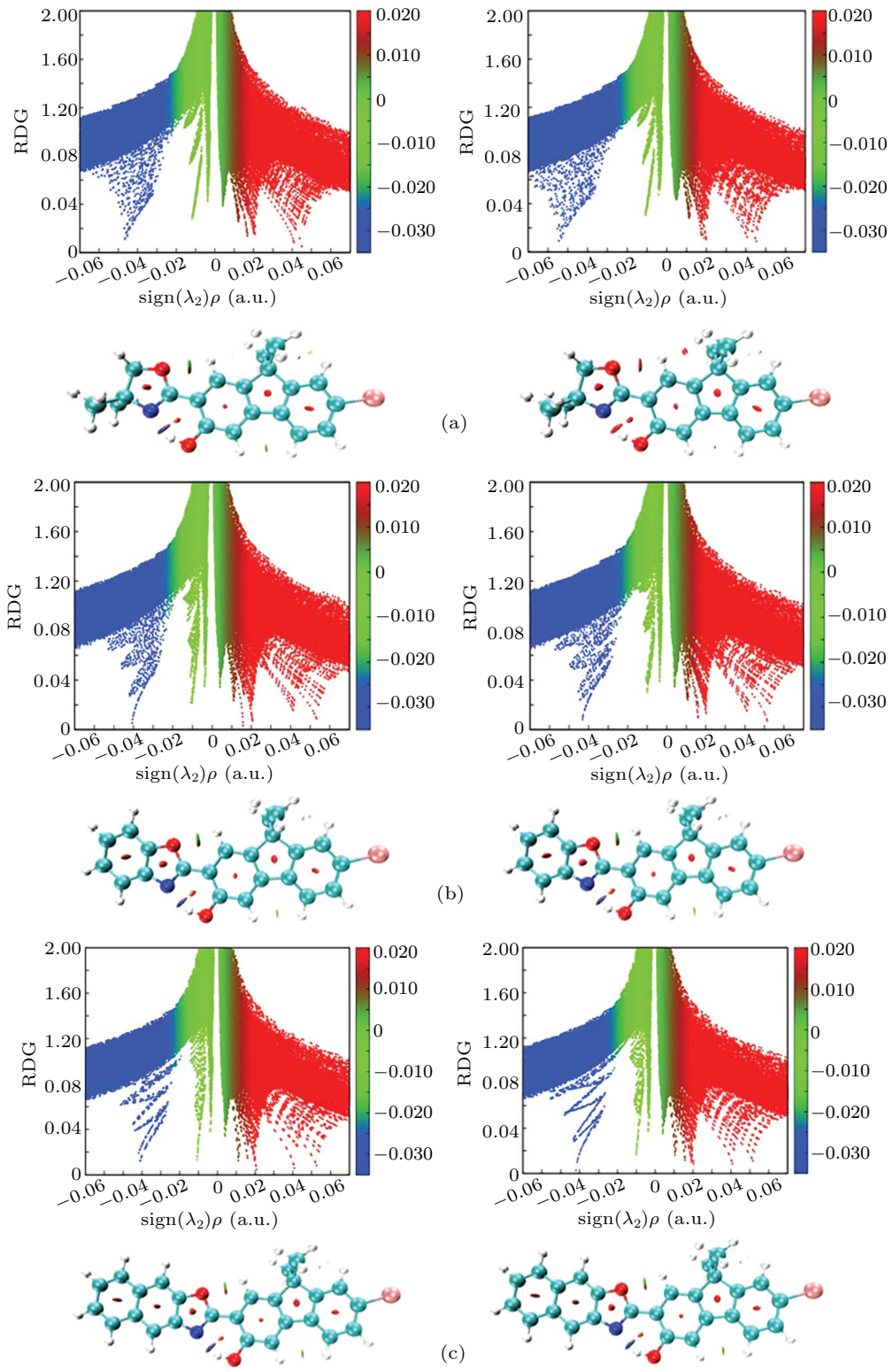


Fig. 5. RDG versus sign(λ_2)ρ and low-gradient isosurfaces for Oxa–OH, BO–OH and NO–OH configurations. Weak interactions can be detected according to RDG.

3.4. Potential energy curves

To further discuss the effect of different substituents on the ESIPT process of Oxa–OH, BO–OH, and NO–OH, the PESs in the S_0 and S_1 states were provided by the DFT and TDDFT methods, which are displayed in Fig. 6. Besides, the O–H bond length ranges from 0.99 Å to 1.99 Å with a step size of 0.1 Å. It can be found that their barrier height in the S state is 9.5 kcal/mol, 10.1 kcal/mol, and 9.8 kcal/mol. It asseverates that it is demanding for these configurations to spontaneous PT in ground state. When the excited molecule transmits to the S_1 state, we found that the barrier height of the Oxa–OH, BO–OH, and NO–OH in chloroform solvent dropped to 1.4 kcal/mol, 6.1 kcal/mol, and 7.4 kcal/mol, re-

spectively. Evidently, the ESIPT reaction is more likely to take place in the S_1 state. Even more noteworthy, the barrier height of BO–OH and NO–OH increase when adding π-conjugation-substitution, while the calculated peak of enol and keto fluorescence of NO–OH is distinctly bathochromic-shift relative to the Oxa–OH configuration. In addition, the inverse reaction of ESIPT with three different substitutional configurations has to overcome a much higher energy barrier than the forward reaction. Therefore, we believe that the reverse ESIPT reaction cannot be spontaneous.

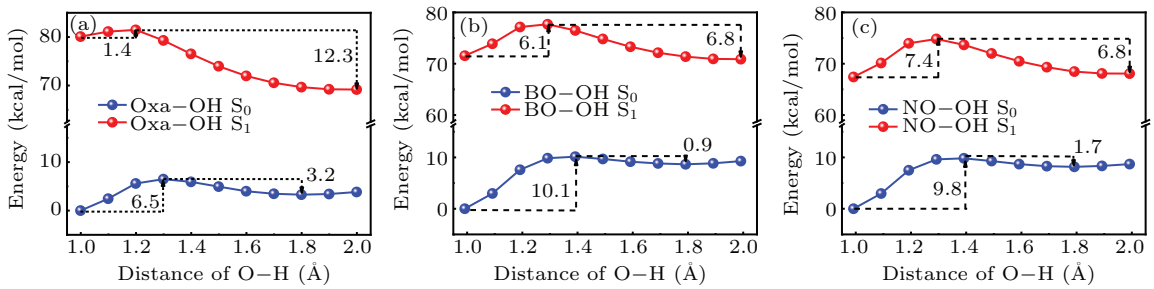


Fig. 6. Potential-energy curves of S_1 and S_0 states for (a) Oxa–OH, (b) BO–OH and (c) NO–OH as functions of the O–H bond length.

4. Conclusions

In this paper, the influence of different π-conjugation-substitutions on ESIPT and photophysical properties have been investigated in chloroform solvent by the DFT and TDDFT methods. Through the analysis of bond length, bond angle and infrared vibration spectrum, it indicates that the hydrogen bonding interaction in excited state is strengthened, which is beneficial to the ESIPT processes. Interestingly, the barrier height of NO–OH is higher when adding π-conjugation-substitution, while the calculated peak of enol and keto fluorescence of NO–OH is distinctly bathochromic-shift relative to the Oxa–OH configuration, which means that the π-conjugation-substitution can diversify the fluorescence color.

Acknowledgements

Project supported by the National Natural Science Foundation of China (Grant No. 11974152), the Shenyang High level Innovative Talents Program (Grant No. RC200565), the Science program of Liaoning Provincial Department of Education (Grant No. LJKZ0097), the Intercollegiate cooperation project of colleges and universities of Liaoning Provincial Department of Education.

References

[1] Yu F B, Li P, Li G Y, Zhao G Y, Chu T S and Han K L 2011 *J. Am. Chem. Soc.* **133** 11030
[2] Li Y Z, Li Y C, Song P, Ma F C, Liang J P and Sun M T 2017 *Rsc. Adv.* **7** 20520
[3] Alyaninezhad Z, Bekhradnia A, Feizi N, Arshadi S and Zibandeh M 2019 *Spectrochim. Acta, Part A.* **212** 32
[4] Pallavi P, Kumar V, Hussain M W and Patra A 2018 *ACS Appl. Mater. Interfaces* **10** 44696
[5] Sun M T 2006 *J. Chem. Phys.* **124** 6049
[6] Zhao J, Dong H and Zheng Y 2018 *J. Phys. Chem. A* **122** 1200
[7] Zhou Q, Du C, Yang L, Zhao M Y, Dai Y M and Song P 2017 *J. Phys. Chem. A* **121** 4645
[8] Weller A 1955 *Naturwissenschaften* **42** 175
[9] Kukura P, McCamant D W and Mathies R A 2007 *Rev. Phys. Chem.* **58** 461
[10] Chou P T, Chen Y C, Yu W S, Chou Y H, Wei C Y and Cheng Y M 2001 *J. Phys. Chem. A* **105** 1731
[11] Ameer-Beg S, Ormson S M, Brown R G, Matousek P, Towrie M, Nibbering E T J, Foggi P and Neuwahl F V R 2001 *J. Phys. Chem. A* **105** 3709
[12] Lim S J, Seo J and Park S Y 2006 *J. Am. Chem. Soc.* **128** 14542
[13] Wei Q and Zhou Q 2017 *J. Lumin.* **83** 7
[14] Liu X C, Yin H, Li H and Shi Y 2017 *Acta Part A* **177** 1
[15] Cardoso M B, Samios D, da Silveira N P, Rodembusch F S and Stefani V 2007 *Photochem.Photobiol. Sci.* **6** 99
[16] Sun L, Chen Y and Sun M T 2021 *J. Phys. Chem. C* **126** 487
[17] Keshav K, Kumawat M K, Srivastava R and Ravikanth M 2017 *Mater. Chem. Front.* **1** 1207
[18] Wang D J, Fan X P, Sun S G, Du S Z, Lia H J, Zhu J L, Tang Y F, Chang M X and Xu Y Q 2018 *Sensors Act. B* **264** 304
[19] Tordo A, Jeanneau E, Bordy M, Bretonnière Y and Hasserodt J 2021 *J. Mater. Chem. C* **9** 12727
[20] Gobel D, Rusch P, Duvinage D, Bigall N C and Nachtsheim B J 2020 *Chem. Commun.* **56** 5430
[21] Chlegel H B 1982 *J. Comput. Chem.* **3** 214
[22] Su S and Fang H 2020 *Spectrochim Acta A Mol. Biomol. Spectrosc.* **233** 118214
[23] Frisch M J, Trucks G W, Schlegel H B, *et al.* 2009 Gaussian 09, Revision B. 02; Gaussian, Inc., Wallingford, CT
[24] Becke A D 1993 *J. Chem. Phys.* **98** 5648
[25] Marciniak H, Hristova S, Deneva V, Kamounah F S, Hansen P E, Lochbrunner S and Antonov L 2017 *Phys. Chem. Chem. Phys.* **19** 26621
[26] Vosko S H, Wilk L and Nusair M 1980 *Can. J. Phys.* **58** 1200
[27] Lee C T, Yang W and Parr R G 1988 *Phys. Rev. B* **37** 785
[28] Humphrey W, Dalke A and Schulten K 1996 *J. Mol. Graphics* **14** 33
[29] Lu T and Chen F 2012 *Journal of Computational Chemistry: Organic, Inorganic, Physical, Biological* **33** 580
[30] Barboza C A and Sobolewski A L 2018 *Phys. Chem. Chem. Phys.* **20** 25164
[31] Yu F B, Li P, Wang B S and Han K L 2013 *J. Am. Chem. Soc.* **20** 7674
[32] Zhao G J and Han K L 2012 *Acc. Chem. Res.* **45** 404
[33] Wang H B, Zhao D P, Song P, Ma F C and Li Y Z 2020 *J. Mol. Liq.* **303** 112594
[34] Li D L, Li C Z and Liu Y F 2016 *J. Mol. Liq.* **218** 670
[35] Chen J R, Yu T, Ubba E, Xie Z L, Yang Z Y, Zhang Y, Liu S W, Xu J R, Aldred M P and Chi Z G 2019 *Adv. Opt. Mater.* **7** 1801593
[36] Borole A P and Lewis A J 2017 *Sustainable Energy Fuels.* **1** 725
[37] Han J H, Cao B F, Zhang X, Su X, Diao L H, Yin H and Shi Y 2020 *J. Mol. Liq.* **306** 112894
[38] Li Y, Liu X C, Han J H, Cao B F, Sun C F, Diao L H, Yin H and Shi Y 2019 *Acta Part A* **222** 117244